

Target-included model and hybrid decoding of stereotyped hand movement in the motor cortex

Wei Wu* and Nicholas G. Hatsopoulos

Abstract—A number of decoding methods, varying from common linear Gaussian models to more complicated point process frameworks, have been developed to infer hand movement from neuronal firing activity in the motor cortex. Most of these methods focus on estimating subject's hand trajectory in a continuous movement. We recently proposed a template-based time identification decoding approach and showed that if a stereotyped movement is well represented by a sequence of targets (or landmarks), then the main structure of the movement will be better addressed by detecting the reaching times at those targets. Both trajectory decoding and landmark-time decoding have advantages respectively, whereas a coupling of these two different strategies has not been examined. Here we propose a synergy that comes from combining these two approaches for a stereotyped movement under a state-space framework, where the recordings were made in the arm area of primary motor cortex in an awake behaving monkey using a chronically implanted multi-electrode array. We at first identify the target times using the template-based method. Then we include the detected targets as a linear control input in the kinematic model of the state-space formulation. Such an inclusion is justified by the empirical linear relationship between the kinematics and target positions. Experimental results show that the hybrid model includes the benefits from both approaches and significantly improves the decoding accuracy.

I. INTRODUCTION

Recent neural decoding models have been demonstrated useful in estimating continuous kinematic parameters such as hand movement trajectory. The models include linear regressions [1], [2], Kalman filters [3], particle filters [4], point process frameworks [5], [6], model-based maximum likelihood [7], artificial neural networks [8], mixture trajectory models [9], and general purpose filter [10]. These methods focus on estimating the entire movement trajectory, and we refer to them as trajectory decoding methods. In contrast, if a movement can be well represented by certain landmark points, these trajectory decodings may not appropriately characterize the essential structure of the movement [11]. To investigate the coding in such type of movement, we recently designed an experimental paradigm by letting the monkey's hand pass through a sequence of targets that appeared on the four corners of a square in counterclockwise order [11]. Based on this experiment, we developed an identification

algorithm which accurately detected the reaching time at each target. We showed that the time decoding method provides a more reasonable reconstruction of the stereotyped movement than a trajectory decoding model.

In general, both trajectory decoding and time decoding have advantages, respectively. The time decoding can reconstruct the main structure, while it lacks the details between landmarks. In contrast, the trajectory decoding can reasonably reconstruct each point, while it is often difficult to identify the main structure in a landmark-defined trajectory. Focusing on a more appropriate neural representation for target-directed movement, we propose to combine these two methods to exploit the benefits from them. To achieve this goal, we propose to build a target-included model where the target information is utilized in the decoding process. Our approach follows a state-space framework which is preferred in current neural coding in the motor cortex [4], [5], [3]. State-space models often focus on an appropriate representation of neural activity by the likelihood model, and use a simple autoregressive prior to describe the hand motion over time. Recent studies have utilized the target information in the model, while they only used it as the end point of the autoregressive movement [12], [13], [9]. The models are still based on the assumption that there is no external influence to the behavior. This assumption, however, is not appropriate as the subjects' actual movements were always target-directed. The voluntary movement would be more properly characterized if the target information is incorporated into the kinematic model.

In this manuscript, we at first examine the relationship between kinematics and target from an experimental recording where they were both continuously distributed over the workspace. Empirical investigation shows that the kinematics are approximately a linear function of the target positions. Based on this result, we propose to add the target position as a linear control term to the autoregressive kinematic model. To examine the new model in neural decoding, we use a linear Gaussian likelihood to represent the distribution of firing rates conditioned on the kinematics. The new kinematic prior and the likelihood constitute a Kalman filter model [3], an efficient and accurate decoding system that has been used in on-line, closed-loop neural control experiments in monkey subjects and human patients [14], [15]. To distinguish the current and previous Kalman filters, we refer to the new method as a target-included Kalman filter (TIKF) and the previous one as a control-free Kalman filter (CFKF). The difference between these two models is that the CFKF does not include any control term in the autoregressive prior, while

This work is supported by an FSU Planning grant to WW and an NIH-NINDS grant R01 NS45853 to NGH.

*WW is with the Department of Statistics, Florida State University, 117 N. Woodward Ave, Tallahassee, FL 32306-4330, USA (email: wwu@stat.fsu.edu).

NGH is with the Department of Organismal Biology and Anatomy, Committees on Computational Neuroscience and Neurobiology, University of Chicago, 1027 E. 57th St, Chicago, IL 60637, USA (email: nicho@uchicago.edu).

the TIKF does so by including the target. As the target is linearly included, the prior model remains linear, and thus the efficient Kalman filter algorithm can still be fully utilized in the decoding process.

Using the proposed TIKF model, we build the hybrid decoding of stereotyped hand movement in two steps: 1. Detect landmarks by the template-based identification method. 2. Incorporate the detected landmarks to the prior of an TIKF model, and then decode the neural firing rates using a Kalman filter algorithm. Focusing on the estimation accuracy, we further examine the decoding using a Kalman smoother, an off-line method which uses all neural activity (past, current, and future) in the estimation.

II. METHODS

A. Experimental Methods

Electrophysiological recording. The neural data used here were previously recorded and have been described elsewhere [16], [11]. Briefly, silicon microelectrode arrays containing 100 platinized-tip electrodes were implanted in the arm area of primary motor cortex (MI) in two juvenile male macaque monkeys (*Macaca mulatta*). Signals were filtered, amplified (gain, 5000) and recorded digitally (14-bit) at 30 kHz per channel using a Cerebus acquisition system (Cyberkinetics Inc.). Single units were manually extracted by the Contours and Templates methods using Offline Sorter. The number of units in each electrode varied from one to five. The monkeys were trained to perform behavioral tasks by moving a cursor to targets via contralateral arm movements in the horizontal plane.

Random Target Pursuit (RTP) task – Monkey 1. At any one time, a single target appeared at a random location in the workspace, and Monkey 1 was required to reach it within 2 seconds. As soon as the cursor reached the target, the target disappeared and a new target appeared in a new, pseudo-random location (Fig. 1A). After reaching the seventh target, the monkey was rewarded with a drop of water or juice. A new set of seven random targets was presented on each trial. The majority of trials were 4-5 seconds in duration. The monkey successfully completed 400 trials, where 125 MI single cells were simultaneously recorded. The firing rates of these cells were computed by counting the number of spikes within the previous 50 ms time window. To match time scales, the hand positions were also sampled every 50 ms. We computed hand velocity and acceleration using simple differencing on position. We also recorded the time instant when each target was reached.

Square-Path (SP) task – Monkey 2. In contrast to the RTP task, the targets in the SP task are all fixed at the four corners of a square and the movement is stereotyped (Fig. 1B). In this experiment, a landmark event was defined as the cursor reaching any of the corners of the square that also corresponded to the time at which the next target appeared. A movement sequence started at the time when the first corner was reached. A trial could start at any time after the end of the previous one. At the start of a trial, the target appeared at the upper right corner of the square and the

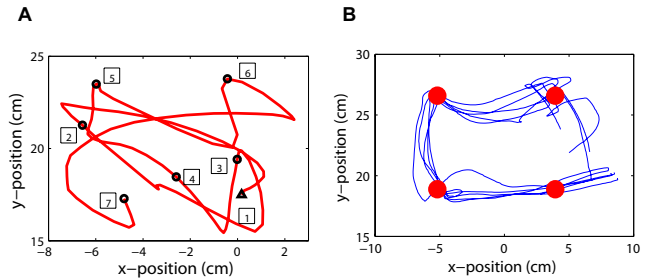


Fig. 1. Two behavioral tasks used in this study. **A.** Trajectory of hand movement in one sample trial of the RTP task. The hand started at the first target (small triangle), and then moved to reach each subsequent target (small circle). The trial was complete when the seventh target was reached. **B.** Trajectories of hand movement in five successful trials of the SP task. In each of the trials, the monkey’s hand passed the four corners of a square in counterclockwise order to reach a target that jumped from one corner to another, starting from the upper right corner. The time when the upper right corner was reached was defined as the onset of the movement sequence in a trial. The corners of the square are denoted by red spots.

monkey had to move the cursor to it. Once reached, the target jumped counterclockwise to the next corner and the monkey had to move the cursor again, and so on (Fig. 1B). A trial was registered as successful only if the monkey reached the target at all of the four corners within 5 seconds. In the data we collected, there were 240 successful trials. A total of 49 MI single units were recorded simultaneously. To use the template-based identification method [11], the bin size is chosen as 10 ms for both firing rates and hand kinematics.

B. Statistical Methods

The statistical methods include two steps: 1. Improve kinematic representation by including target in the prior of a TIKF model. This investigation is based on dataset 1 where the target is distributed over the workspace. 2. Develop a method for coupling the time decoding and trajectory decoding. This study is based on dataset 2 where the monkey’s hand movement follows a fixed pattern by passing through a sequence of landmark points. Our goal is to identify the landmarks first, and then incorporate the detected landmarks in the target-included prior model.

1) *Target-Included Kinematic Model:* In recent Bayesian models, the hand kinematics is often represented as an autoregressive process in the prior term; that is,

$$\mathbf{x}_k = \mathbf{A}\mathbf{x}_{k-1} + \mathbf{w}_k. \quad (1)$$

where $\mathbf{x}_k = [x, y, v_x, v_y]^T_k$ represents x -position, y -position, x -velocity, and y -velocity at time $t_k = k\Delta t$ ($\Delta t = 50ms$ in dataset 1), $\mathbf{A} \in \mathbb{R}^{4 \times 4}$ is the linear coefficient matrix. The noise terms \mathbf{w}_k are assumed zero mean and normally distributed, i.e. $\mathbf{w}_k \sim N(0, \mathbf{W})$, $\mathbf{W} \in \mathbb{R}^{4 \times 4}$. Equation 1 is based on the assumption that the monkey’s hand moved in the horizontal plane without any external influence. This assumption nicely addresses the continuity of the movement while it lacks a description of the nature of the target-directed movement. The subject’s hand movement (e.g. RTP task) was not freely moving in the plane, but was always directed by a target on the projection surface.

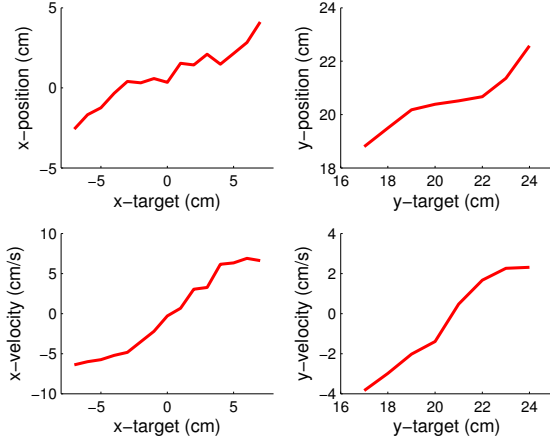


Fig. 2. Correlations between kinematics and target in dataset 1: The upper two panels show averaged x -position and y -position as a function of x -target and y -target, respectively; The lower two panels show averaged x -velocity and y -velocity as a function of x -target and y -target, respectively.

Correlations between kinematics and target. Here we investigate the effect of target on the representation of kinematics over time. At first, we examine the tuning function between the hand position and target. We use dataset 1 (RTP task) where the target covers a continuous region of the workspace. It is found that the position in either coordinate can be approximated as a linear function of the target in the same coordinate (see the upper panels in Fig. 2). This observation is reasonable as the monkey’s hand movement was always towards the target. Likewise, we find a linear approximation between the hand velocity and the target (see the lower panels in Fig. 2). Statistical analysis supports the goodness of the linear fit (multiple regression, t -test, $p < 0.01$ in each fit). Note that we also test the relationship between the hand acceleration and the target, but do not observe any linear trend. Taking into account the relatively insignificant contribution of acceleration in the Kalman filter model [3], we exclude it in the current study; that is, we only use the position and velocity to describe the hand kinematics.

The target-directed prior model. As both position and velocity are strongly correlated with the target, it is critically important to incorporate the target in the characterization of the hand movement. We propose to add the target as a linear control input to the prior model in Equation 1. Then, the new kinematic model is described using the following equation:

$$\mathbf{x}_k = \mathbf{A}\mathbf{x}_{k-1} + \mathbf{B}\mathbf{g}_k + \mathbf{w}_k, \quad (2)$$

where $\mathbf{g}_k = [g_x, g_y]^T$ represents x - and y -target position at time t_k , and $\mathbf{B} \in \mathbb{R}^{4 \times 2}$ is the linear coefficient matrix. As compared to Equation 1, Equation 2 includes a new term for the target, \mathbf{g}_k . We find this term is statistically significant (multiple regression, t -test, $p < 0.01$). This indicates that the new prior provides a more appropriate representation of the target-directed movement.

The Box-Cox transformation. In Equation 2, we incorporate the target into the prior model as a linear control term. To

investigate the appropriateness of the linear inclusion, we use a Box-Cox transformation on the target which is a standard approach to determine whether a non-linear transformation is necessary on the variables in a linear model [17]. Here the target \mathbf{g} is transformed to:

$$h_\lambda(\mathbf{g}) = \begin{cases} \frac{\mathbf{g}^\lambda - 1}{\lambda} & \lambda \neq 0 \\ \log \mathbf{g} & \lambda = 0 \end{cases}$$

where λ is the parameter in the transformation and is often taken in the range $[-2, 2]$. Using the transformed target, the prior model is described as:

$$\mathbf{x}_k = \mathbf{A}\mathbf{x}_{k-1} + \mathbf{B}h_\lambda(\mathbf{g}_k) + \mathbf{w}_k. \quad (3)$$

We look for the optimal $\hat{\lambda}$ which maximizes the probability $p_\lambda(\mathbf{X}_M | \mathbf{G}_M)$, where \mathbf{X}_M and \mathbf{G}_M represent kinematics and targets in the entire training set, respectively. If $\hat{\lambda}$ is around 1, then such a transformation is nearly linear and therefore not necessary. Otherwise, a transformation with $\lambda = \hat{\lambda}$ would lead to a more appropriate representation of target-directed hand movement.

Target-include Kalman filter. The Kalman filter is a well known Bayesian inference system and is formulated in terms of a likelihood and a prior. The likelihood term uses a linear Gaussian model to describe the relationship between firing rates and hand motion. It is described using the following equation:

$$\mathbf{z}_k = \mathbf{H}\mathbf{x}_k + \mathbf{q}_k, \quad (4)$$

where $\mathbf{x}_k = [x, y, v_x, v_y]^T$ represents x -position, y -position, x -velocity, and y -velocity at time t_k , and $\mathbf{z}_k \in \mathbb{R}^C$ represent a $C \times 1$ vector containing the firing rates at time t_k for C observed neurons. $\mathbf{H} \in \mathbb{R}^{C \times 4}$ is the linear coefficient matrix. The noise terms \mathbf{q}_k are assumed zero mean and normally distributed, i.e. $\mathbf{q}_k \sim N(0, \mathbf{Q})$, $\mathbf{Q} \in \mathbb{R}^{C \times C}$.

The likelihood in Equation 4 and the prior in Equation 1 constitute an Kalman filter model. As there is no target included in the prior, this is a CFKF model. In contrast, this likelihood and the new prior in Equation 2 constitute a TIKF model which utilizes the nature of the target-directed movement. The identification of the CFKF model has been discussed in our previous work [3]. Analogously, the parameters $\mathbf{A}, \mathbf{B}, \mathbf{W}, \mathbf{H}, \mathbf{Q}$ in the TIKF model can also be identified using the maximum likelihood estimation. The detailed procedure is described in the Appendix.

After the parameters in the TIKF model are identified, the hand kinematics can be inferred from neural activity using a Kalman filter algorithm. Focusing on the estimation accuracy, we also decode neural activity using a Kalman smoother [18]. This method has the same model as a Kalman filter, whereas the decoding at each step is based on the overall neural activity (past, current, and future). To be consistent with the Kalman filters, we refer to the regular Kalman smoother as a CFKS method, and the target-included Kalman smoother as a TIKS method. The detailed decoding process of TIKF and TIKS is also described in the Appendix.

TABLE I
AVERAGED DECODING ACCURACY FOR THE RTP TASK

Method	CC	$MSE(cm^2)$
CFKF	(0.87,0.85)	7.7
TIKF	(0.91,0.88)	5.3
CFKS	(0.90,0.88)	6.4
TIKS	(0.92,0.90)	5.0

2) Coupling the Time Decoding and Trajectory Decoding:

For a target-directed movement, we propose to include the target in the kinematic model (Equation 2). The inclusion is based on the assumption that the target is known before the movement. However, this precondition may not be necessary in certain experimental paradigms. If the target only appears at certain sequential fixed positions (e.g. in the SP task), our recently developed method can detect the time when each target is reached using population neuronal activity [11]. Using this idea, we incorporate the detection result into the prior (kinematic) term of a TIKF model. The coupled model utilizes the benefits from both time decoding and trajectory decoding and is expected to provide a more accurate decoding.

Add the detected landmarks to the trajectory decoding model. Let the positions of n landmarks in a certain type of behavior be M_1, M_2, \dots, M_n . Assume the occurrence times of all landmarks have been identified. We denote them as $\hat{t}_1, \hat{t}_2, \dots, \hat{t}_n$. Then the target at each time is calculated as,

$$\hat{\mathbf{g}}_k = \begin{cases} M_1, & \text{if } t_k < \hat{t}_1 \text{ or } t_k \geq \hat{t}_n \\ M_{i+1}, & \text{if } \hat{t}_i \leq t_k < \hat{t}_{i+1} \end{cases} \quad (5)$$

Using the above identified target, the new kinematic model is modified as:

$$\mathbf{x}_k = \mathbf{A}\mathbf{x}_{k-1} + \mathbf{B}\hat{\mathbf{g}}_k + \mathbf{w}_k. \quad (6)$$

This equation is the same as Equation 2 except that the target $\hat{\mathbf{g}}_k$ at each time t_k is estimated from the identification method. Equations 4 and 6 constitute a TIKF model. Hence, the decoding can also be performed using a Kalman filter algorithm or a Kalman smoother algorithm.

III. RESULTS

A. The RTP Task

There are 400 trials in total in dataset 1 (RTP task). We took the first 100 trials as the training set, which is around 8 minutes long and provides sufficient samples to identify the parameters. Then we decoded the firing rates to reconstruct the hand trajectories in the remaining testing set (300 trials).

Decoding. We used the correlation coefficient, CC , and mean squared error, MSE , to measure decoding accuracy in each testing trial. The decoding results are summarized in Table I. On average the TIKF decreases the MSE in the CFKF by about 31% and increases the CC by about 4% (note that the CC s in the CFKF are already close to the upper limit 1). Likewise, on average the TIKS decreases the MSE in the CFKS by about 22% and increases the CC by about 2%. These results indicate that the target-included

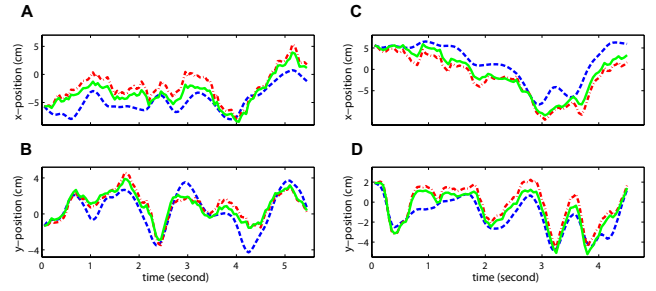


Fig. 3. Reconstruction examples of the RTP task: **A.** True x -position (dashed blue) of one test trial and its reconstructions using the CFKF method (dashdot red) and the TIKF method (solid green). **B.** Same as A except for the y -position. **C.** True x -position (dashed blue) of another test trial and its reconstructions using the CFKS method (dashdot red) and the TIKS method (solid green). **D.** Same as C except for the y -position.

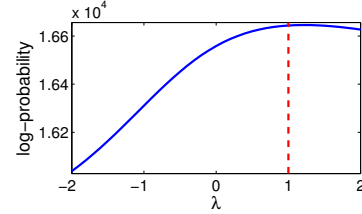


Fig. 4. The Box-Cox transformations on the target. The solid line denotes the log-probability as a function of λ . The dashed line denotes the log-probability at $\lambda = 1$.

models significantly improve decoding accuracy over the regular models. The improved performance is illustrated by a few decoding examples (Fig. 3).

The Box-Cox transformation. For each $\lambda \in \{-2, -1.9, -1.8, \dots, 2\}$, we estimated the parameters in the model using the training data, and then computed the log-probability, $\log p_\lambda(\mathbf{X}_M | \mathbf{G}_M)$. We plotted the log-probability as a function of λ (Fig. 4). The result indicates that the maximum log-probability is obtained when λ is around 1. This shows that the commonly used Box-Cox transformation (Equation 3) is not necessary, and the linear inclusion of the target in Equation 2 would fit the data well.

B. The SP Task

The decoding in the RTP task shows that including target can significantly improve the decoding accuracy. In the SP task, the movement was well-defined by the times when the four corners are reached. Over the 240 trials, we took the first 200 trials as the training set, and the remaining 40 as the testing set.

Coupling the time decoding and trajectory decoding. Using the recently proposed identification method, we found that over the 40 test trials, 29 of them can be accurately detected where the averaged error was only 0.223 ± 0.200 second (over four corners) [11]. As the target only appeared at the fixed four corners of the square, we obtained the target position at each time using Equation 5. Then the detected target was incorporated into the kinematic model (Equation 6). The new prior, Equation 6, and the linear Gaussian likelihood, Equation 4, constitute a TIKF model with estimated

TABLE II
AVERAGED DECODING RESULTS FOR THE SP TASK

Method	CC	$MSE(cm^2)$
CFKF	(0.93,0.92)	7.1
TIKF with estimated target	(0.94,0.93)	6.3
CFKS	(0.95,0.94)	6.1
TIKS with estimated target	(0.95,0.95)	5.7

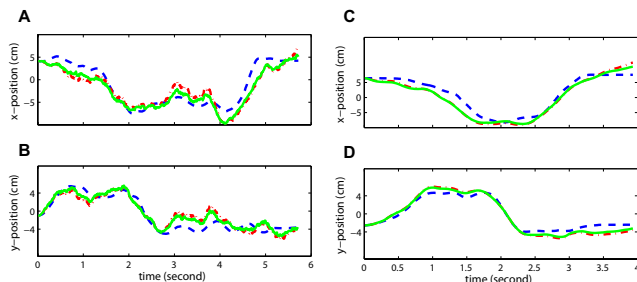


Fig. 5. Reconstruction examples of the SP task: **A.** True x -position (dashed blue) of one test trial and its reconstructions using the CFKF method with estimated target (dashdot red) and the TIKF method with estimated target (solid green). **B.** Same as **A** except for the y -position. **C.** True x -position (dashed blue) of another test trial and its reconstructions using the CFKS method with estimated target (dashdot red) and the TIKS method with estimated target (solid green). **D.** Same as **C** except for the y -position.

target. Here we compared the decoding performance of this TIKF with that of the CFKF for the 29 trials where the target times are not used. Experimental results are summarized in Table II. On average the TIKF with estimated target decreases the MSE in CFKF by about 11%. Likewise, on average the TIKS decreases the MSE in CFKS by about 7%. In contrast to the MSE , the improvement on CC is less insignificant. This is largely due to the fact that CC in each method is already very close to the upper limit 1. The improved performance of the target-included models is illustrated by a few decoding examples (Fig. 5).

Note that in this decoding the target at each time is not pre-known, but identified from the neural activity. This is an improvement over the decoding in the RTP task where the target information needs to be given. The proposed hybrid model utilized the stereotyped nature of the SP movement, and provided a more powerful decoding system.

IV. DISCUSSION

State-space models often use a linear autoregressive prior to describe the hand motion over time [4], [5], [3]. Such a representation is based on the assumption that there is no external influence to the behavior. This assumption, however, is not appropriate as the subjects' actual movements are all target-directed. Several research groups have made significant progress by utilizing the target information under a Bayesian framework. A simulation study by Srinivasan and colleagues [13] included a static target in the model by assuming an autoregressive prior with known target position and arrival time. The method was recently improved to an efficient, non-recursive way by Kulkarni and Paninski [12]. Yu and colleagues [9] took the advantage of the finite number of target locations in their center-out reaching experiment,

and modeled the movement to each target independently as an autoregressive process. Kemere and Meng [19] included the target in feed-forward-controlled linear systems, where the target was actually used in the likelihood model instead of the kinematic prior model. In contrast to these studies, we propose to add the target position as a linear control term to the autoregressive kinematic model. This is motivated by the approximately linear relationship between kinematics (position and velocity) and target position. One advantage in our model is that the arrival time at the target does not need to be known (which is needed in [13] and [12]). The new kinematic model coupling a linear Gaussian likelihood constitutes a TIKF model. Experimental results show that the TIKF model not only improves the representation of kinematics, but also provides more accurate decoding than a classical CFKF model.

Our recent work showed that for a landmark-defined movement both time decoding and trajectory decoding have advantages, respectively [11]. A time decoding can reconstruct the main structure, while it lacks the details between landmarks. In contrast, a trajectory decoding can reconstruct each point in the movement, while it is difficult to identify the main structure of a landmark-defined trajectory. Focusing on a more appropriate neural representation, we propose to combine these two different decoding methods to fully exploit the benefits from them. Experimental results show that such a combination is effective as more accurate decoding is obtained based on the same neural activity. However, we note that the identification method is only an off-line method in that all neural activity (past, current, and future) is used in the time decoding process. An on-line identification would be desirable for future neural prosthetic applications.

V. CONCLUSIONS AND FUTURE WORK

In this paper we have presented a hybrid decoding system, TIKF, by including estimated target in the prior of the Kalman filter model. We focus on providing more appropriate description of the target-directed two-dimensional hand movement, and utilize the benefits from both timing decoding and trajectory decoding. The new model includes the target as a control input based on the approximately linear relationship between kinematics and target position. Experimental results show that the hand movement is more appropriately represented in the new model. We further compared the decoding performance of the proposed TIKF (with estimated target) and the previous CFKF model, and found that the new method substantially improves the decoding accuracy.

Focusing on more accurate representation of neural activity, our future work will explore other Bayesian formulations where the likelihood can be any non-linear equations such as Poisson models or mixture models. A non-linear likelihood and the target-included prior constitute a more general state-space model. We will also study the inclusion of goal using a non-Bayesian formulation, such as a linear regression or neural network. Finally, the current timing decoding is an off-line method as all neural signals are used to identify the targets. We will explore an on-line identification method

where only the past and current neural activity is used. Such an on-line approach would provide feasible control of robotic limbs in neural motor prosthetics.

ACKNOWLEDGMENT

We thank S. Francis, Z. Haga, D. Paulsen, and J. Reimer for training the monkeys and collecting the data.

REFERENCES

- [1] J. M. Carmena, M. A. Lebedev, R. E. Crist, J. E. O'Doherty, D. M. Santucci, D. F. Dimitrov, P. G. Patil, C. S. Henriquez, and M. A. L. Nicolelis, "Learning to control a brain-machine interface for reaching and grasping by primates," *PLoS, Biology*, vol. 1, no. 2, pp. 001–016, 2003.
- [2] L. R. Hochberg, M. D. Serruya, G. M. Friehs, J. A. Mukand, M. Saleh, A. H. Caplan, A. Branner, R. D. Chen, D. Penn, and J. P. Donoghue, "Neuronal ensemble control of prosthetic devices by a human with tetraplegia," *Nature*, vol. 442, pp. 164–171, 2006.
- [3] W. Wu, Y. Gao, E. Bienenstock, J. P. Donoghue, and M. J. Black, "Bayesian population decoding of motor cortical activity using a Kalman filter," *Neural Computation*, vol. 18, no. 1, pp. 80–118, 2006.
- [4] A. E. Brockwell, A. L. Rojas, and R. E. Kass, "Recursive bayesian decoding of motor cortical signals by particle filtering," *Journal of Neurophysiology*, vol. 91, pp. 1899–1907, 2004.
- [5] U. Eden, W. Truccolo, M. R. Fellows, J. P. Donoghue, and E. M. Brown, "Reconstruction of hand movement trajectories from a dynamic ensemble of spiking motor cortical neurons," in *Proc. IEEE EMBS*, September 2004, pp. 4017–4020.
- [6] W. Truccolo, U. Eden, M. Fellows, J. Donoghue, and E. Brown, "A point process framework for relating neural spiking activity to spiking history, neural ensemble and extrinsic covariate effects," *Journal of Neurophysiology*, vol. 93, pp. 1074–1089, 2005.
- [7] C. Kemere, K. V. Shenoy, and T. H. Meng, "Model-based neural decoding of reaching movements: a maximum likelihood approach," *IEEE Transactions on Biomedical Engineering*, vol. 51, no. 6, pp. 925–932, 2004.
- [8] J. C. Sanchez, D. Erdogmus, J. C. Principe, J. Wessberg, and M. A. L. Nicolelis, "Interpreting spatial and temporal neural activity through a recurrent neural network brain machine interface," *IEEE Transactions on Neural Systems and Rehabilitation Engineering*, vol. 13, pp. 213–219, 2005.
- [9] B. M. Yu, C. Kemere, G. Santhanam, A. Afshar, S. I. Ryu, T. H. Meng, M. Sahani, and K. V. Shenoy, "Mixture of trajectory models for neural decoding of goal-directed movements," *Journal of Neurophysiology*, vol. 97, pp. 3763–3780, 2007.
- [10] L. Srinivasan, U. T. Eden, S. K. Mitter, and E. N. Brown, "General-purpose filter design for neural prosthetic devices," *Journal of Neurophysiology*, vol. 98, pp. 2456–2475, 2007.
- [11] Z. Chi, W. Wu, Z. Haga, N. Hatsopoulos, and M. D., "Template-based spike pattern identification with linear convolution and dynamic time warping," *Journal of Neurophysiology*, vol. 97, pp. 1221–1235, 2007.
- [12] J. E. Kulkarni and L. Paninski, "State-space decoding of goal directed movement," *IEEE Signal Processing Magazine*, vol. 25, no. 1, pp. 78–86, 2007.
- [13] L. Srinivasan, U. T. Eden, A. S. Willsky, and E. N. Brown, "A state-space analysis for reconstruction of goal-directed movements using neural signals," *Neural Computation*, vol. 18, pp. 2465–2494, 2006.
- [14] W. Wu, A. Shaikhouni, J. P. Donoghue, and M. J. Black, "Closed-loop neural control of cursor motion using a Kalman filter," in *Proc. IEEE EMBS*, September 2004, pp. 4126–4129.
- [15] S. P. Kim, J. Simeral, L. Hochberg, J. P. Donoghue, G. Friehs, and M. J. Black, "Multi-state decoding of point-and-click control signals from motor cortical activity in a human with tetraplegia," in *The third IEEE EMBS Conference on Neural Engineering*, May 2007, pp. 486–489.
- [16] W. Wu and N. Hatsopoulos, "Evidence against a single coordinate system representation in the motor cortex," *Experimental Brain Research*, vol. 175, no. 2, pp. 197–210, 2006.
- [17] J. Faraway, *Linear Models with R*. Chapman & Hall/CRC, 2005.
- [18] S. Haykin, *Adaptive Filter Theory*, 4th ed. Prentice-Hall, 2001.
- [19] C. Kemere and T. H. Meng, "Optimal estimation of feed-forward-controlled linear systems," in *Proc IEEE Int. Conf. Acoustics, Speech and Signal Processing*, vol. 5, 2005, pp. 353–356.

APPENDIX

Identifying the TIKF model. Similar to the identification in [3], the parameters $\mathbf{A}, \mathbf{B}, \mathbf{W}, \mathbf{H}, \mathbf{Q}$ in Equations 2 and 4 can be identified from training data using the maximum likelihood estimation. We assume the hand kinematics $\mathbf{X}_M = [\mathbf{x}_1, \mathbf{x}_2, \dots, \mathbf{x}_M]^T$, target positions $\mathbf{G}_M = [\mathbf{g}_1, \mathbf{g}_2, \dots, \mathbf{g}_M]^T$, and the firing rates $\mathbf{Z}_M = [\mathbf{z}_1, \mathbf{z}_2, \dots, \mathbf{z}_M]^T$ are known for the M time instants in the training set. As the distribution of the target is known, the parameters are identified by maximizing the conditional probability

$$p(\mathbf{X}_M, \mathbf{Z}_M | \mathbf{G}_M).$$

Due to the linear Gaussian structure of the model, this maximization has closed-form solutions:

$$\begin{aligned} \mathbf{A} &= \text{columns 1 to 4 of matrix } \left(\sum_{k=2}^M \mathbf{x}_k \mathbf{y}_k^T \right) \left(\sum_{k=2}^M \mathbf{y}_k \mathbf{y}_k^T \right)^{-1}, \\ \mathbf{B} &= \text{columns 5 to 6 of matrix } \left(\sum_{k=2}^M \mathbf{x}_k \mathbf{y}_k^T \right) \left(\sum_{k=2}^M \mathbf{y}_k \mathbf{y}_k^T \right)^{-1}, \\ \mathbf{W} &= \frac{1}{M-1} \left(\sum_{k=2}^M \mathbf{x}_k \mathbf{x}_k^T - \mathbf{A} \sum_{k=2}^M \mathbf{x}_{k-1} \mathbf{x}_k^T - \mathbf{B} \sum_{k=2}^M \mathbf{g}_k \mathbf{x}_k^T \right), \\ \mathbf{H} &= \left(\sum_{k=1}^M \mathbf{z}_k \mathbf{x}_k^T \right) \left(\sum_{k=1}^M \mathbf{x}_k \mathbf{x}_k^T \right)^{-1}, \\ \mathbf{Q} &= \frac{1}{M} \left(\sum_{k=1}^M \mathbf{z}_k \mathbf{z}_k^T - \mathbf{H} \sum_{k=1}^M \mathbf{x}_k \mathbf{z}_k^T \right). \end{aligned}$$

where $\mathbf{y}_k = [\mathbf{x}_{k-1}^T, \mathbf{g}_k^T]^T \in \mathfrak{R}^6$ denotes the concatenation of kinematics (position and velocity) and target.

The target-included decoding. After the TIKF model is identified, the kinematics can be estimated recursively using a Kalman filter algorithm or a Kalman smoother algorithm [18].

Assuming there are N time steps in a test trial, the Kalman filter algorithm uses the following target-included equations: For $k = 1, \dots, N$, compute

$$\begin{aligned} \hat{\mathbf{x}}_k^- &= \mathbf{A} \hat{\mathbf{x}}_{k-1} + \mathbf{B} \mathbf{g}_k \\ \mathbf{P}_k^- &= \mathbf{A} \mathbf{P}_{k-1} \mathbf{A}^T + \mathbf{W} \\ \mathbf{K}_k &= \mathbf{P}_k^- \mathbf{H}^T (\mathbf{H} \mathbf{P}_k^- \mathbf{H}^T + \mathbf{Q})^{-1} \\ \hat{\mathbf{x}}_k &= \hat{\mathbf{x}}_k^- + \mathbf{K}_k (\mathbf{z}_k - \mathbf{H} \hat{\mathbf{x}}_k^-) \\ \mathbf{P}_k &= (\mathbf{I} - \mathbf{K}_k \mathbf{H}) \mathbf{P}_k^- \end{aligned}$$

where $\hat{\mathbf{x}}_k$ is the Kalman filter estimate at time t_k , and \mathbf{P}_k is its error covariance.

In addition to the above five equations, the Kalman smoother algorithm conducts more calculations as follows: For $k = N$, set $\mathbf{P}_N^s = \mathbf{P}_N$ and $\hat{\mathbf{x}}_N^s = \hat{\mathbf{x}}_N$. Then for $k = N-1, N-2, \dots, 1$, compute

$$\begin{aligned} \mathbf{B}_k^s &= \mathbf{P}_k \mathbf{A}^T \mathbf{P}_{k+1}^- \\ \hat{\mathbf{x}}_k^s &= \hat{\mathbf{x}}_k + \mathbf{B}_k^s (\hat{\mathbf{x}}_{k+1}^s - \hat{\mathbf{x}}_{k+1}^-) \\ \mathbf{P}_k^s &= \mathbf{P}_k - \mathbf{B}_k^s (\mathbf{P}_{k+1}^- - \mathbf{P}_{k+1}^s) (\mathbf{B}_k^s)^T \end{aligned}$$

where $\hat{\mathbf{x}}_k^s$ is the Kalman smoother estimate at time t_k , and \mathbf{P}_k^s is its error covariance.